A&A manuscript no.
(will be inserted by hand later)

Your thesaurus codes are:
01(09.09.1 IC443; 09.19.2; 13.09.4)

ASTRONOMY AND ASTROPHYSICS

ISO–SWS spectroscopy of IC443 and the origin of the IRAS 12 and 25 μm emission from radiative supernova remnants *

E. Oliva[1], D. Lutz[2], S. Drapatz[2], and A.F.M. Moorwood[3],

[1] Osservatorio Astrofisico di Arcetri, Largo E. Fermi 5, I–50125 Firenze, Italy
[2] Max Planck Institute für Extraterrestrische Physik, Postfach 1603, D-85740 Garching, Germany
[3] European Southern Observatory, Karl Schwarzschild Str. 2, D-85748 Garching bei München, Federal Republic of Germany

Received 17 November, accepted 3 December 1998

Abstract. ISO–SWS spectral observations of the supernova remnant IC443 are presented. Like other radiative SNRs, this object is characterized by prominent line–emitting filaments and relatively strong IRAS 12 and 25 μm emission which is commonly interpreted as thermal radiation from very small grains stochastically heated by collisions with the hot plasma behind the shock front. This interpretation is challenged by the data presented in this *Letter* which indicate that most of the 12 and 25 μm IRAS flux is accounted for by ionized line emission (mainly [NeII] and [FeII]). This result also seems to hold for other radiative SNRs. We also discuss the possible contribution of H_2 lines to the IRAS 12 μm flux from the southern rim of IC443 and briefly analyze the element abundances derived from the observed ionic lines.

Key words: ISM: individual objects: IC443; ISM: supernova remnants; Infrared: ISM: lines and bands

1. Introduction

A significant fraction of the galactic supernova remnants were detected by the IRAS satellite (e.g. Arendt 1989, hereafter A89) and their relatively strong FIR emission has been normally interpreted as thermal radiation from dust which is heated by collisions with the hot (million degrees) plasma in the post–shock region (e.g. Braun & Strom 1986, Dwek et al. 1987). This emission could be an important cooling mechanism for non–radiative shocks in young SNRs (e.g. Ostriker & Silk 1973).

The spectral shape of the FIR emission reflects the temperature distribution of the dust which in turn depends on the shock speed and on the density, size and composition of the grains (e.g. Draine 1991). Young SNRs are expected to have a FIR spectrum characterized by a single temperature because, in the hot ($\gtrsim 2\,10^7$ K) plasma typical of these objects, the temperatures of collisionally heated dust grains approach the same value independent of grain size (e.g. Dwek 1987). This is in good agreement with the IRAS data of young SNRs (e.g. Cas A, Tycho, Kepler) whose spectral distributions are fairly well fitted by a single temperature blackbody (e.g. A89)

The IRAS colours of radiative SNRs are much more complex and require an ad hoc combination of dust components of different sizes and temperatures. In particular, the S(12)/S(25) IRAS colours are much bluer than those of young SNRs and require a very large population of very small (< 50 Å) grains (e.g. Arendt et al. 1992). An alternative explanation is that the flux seen in the "blue" IRAS bands is dominated by line emission from the radiative filaments but this possibility could not be verified directly because of the difficulty of measuring the FIR lines prior to ISO. Attempts to estimate the line contamination by extrapolating optical spectral measurements using shock model predictions have led to contradictory conclusions (e.g. Mufson et al. 1986, Arendt et al. 1992).

In this *Letter* we present FIR spectral observations of a prototype radiative SNR which allow a direct comparison between the IRAS and line fluxes. The data are presented in Sect. 2, the results are discussed in Sect. 3 and in Sect. 4 we draw our conclusions.

2. Observations and results

A complete SWS01 (speed 4, 6700 sec total integration time) spectrum centered at α=06^{h}14^{m}32^s.6 δ=22^{o}54' 05" (1950 coordinates) and roughly corresponding to position 1 of Fesen & Kirshner (1980) was obtained on October 16, 1997. The data were reduced using standard routines of the SWS interactive analysis system (IA) using calibration tables as of October 1998. Reduction relied mainly on the default pipeline steps, plus removal of signal spikes, elimination of the most noisy band 3 detectors, and flat–fielding. Note that SWS has a quite high spectral resolution ($R=\lambda/\delta\lambda\simeq 1500$) and is not well suited for measurements of faint continuum fluxes.

Send offprint requests to: E. Oliva

* Based on observations with ISO, an ESA project with instruments funded by ESA Member States (especially the PI countries: France, Germany, the Netherlands and the United Kingdom) and with the participation of ISAS and NASA. The SWS is a joint project of SRON and MPE.

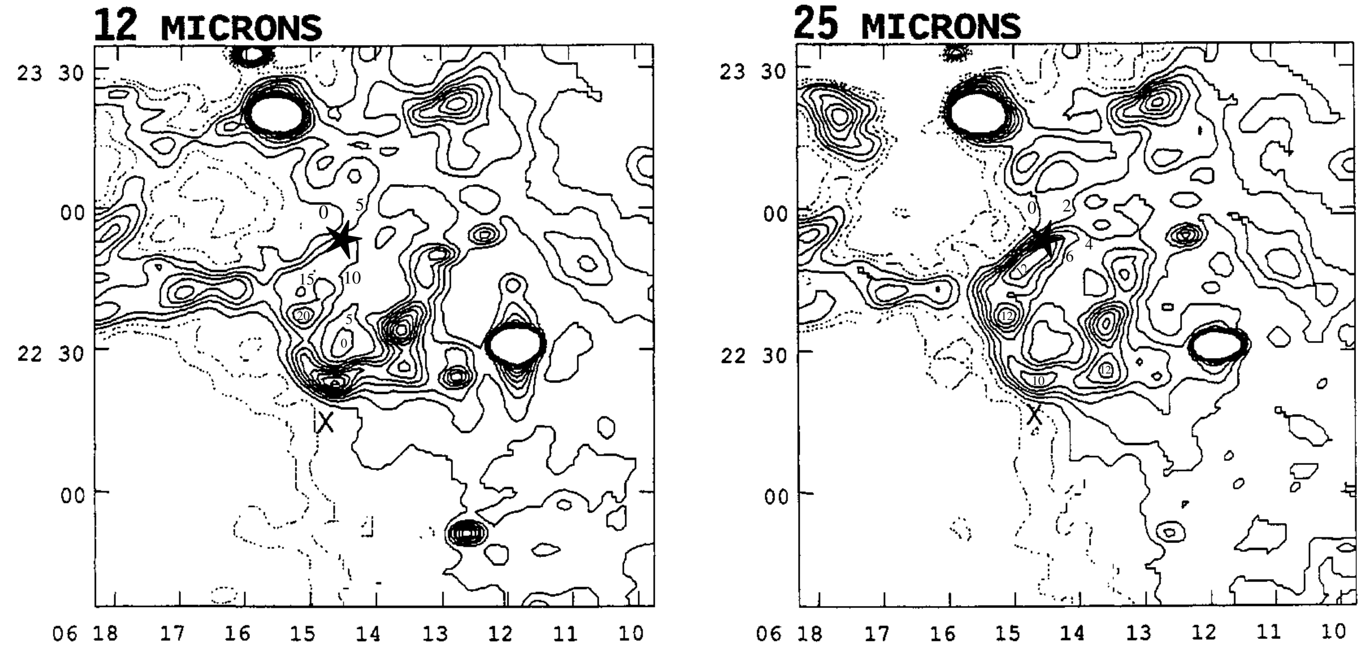

Fig. 1. The position of the SWS aperture (∗) is overlaid onto a reproduction of the IRAS maps of IC443 (adapted from Fig. 30a A89). The solid contours correspond to 0, 5, 10, 15, 20, 25, 30, 35, 40, 45 and 0, 2, 4, 6, 8, 10, 12, 14, 16, 18 ($\times 10^{-8}$ W m^{-2} sr^{-1}) in the 12 and 25 μm bands, respectively. Note that the size of the SWS aperture is much smaller than the symbol used to mark its position.

For the SWS01 mode, in particular, s/n and detector drifts between dark current measurements do not allow measurements of continuum emission at levels much below 1 Jy. The measured IRAS 12 and 25 μm "continuum" fluxes from the SNR would correspond to only $\simeq$0.01 Jy in the SWS aperture and cannot therefore be detected with the spectral observations presented here.

The spectral sections including well detected lines are displayed in Fig. 2 and the derived line fluxes are listed in Table 1 together with their contribution to the IRAS fluxes, estimated using the spectral response shown in Fig. 3. The line profiles are not resolved within the noise (i.e. FWHM<400 km/s), and their centroids are not significantly red/blue–shifted.

The most striking result is that the surface brightness of [NeII]λ12.8 alone is *larger* than that observed by IRAS through the 12 μm filter. This apparent contradiction reflects the somewhat higher spatial resolution of ISO–SWS relative to the undersampled IRAS maps. More specifically, the line emitting filaments visible in the Hα and [SII] images of Mufson et al. (1986) are quite uniformly distributed over many arcmin, i.e. an area larger than the IRAS map resolution, and the average line surface brightness over this area is roughly a factor of 2–4 lower than that within the ISO–SWS aperture. In other words, the ISO spectra, although centered on a bright optical filament, does not sample a spot of exceptionally large line surface brightness, but rather a "typical" line emitting region.

This indicates, therefore, that the IRAS 12 μm "continuum" is indeed dominated by [NeII] line emission, i.e. that this line accounts for at least 50% of the observed IRAS flux. A similar reasoning applies to the IRAS 25 μm flux which is strongly contaminated by emission in the [FeII]λ26.0 ground state transition plus significant contribution from [OIV]λ25.9, [SIII]λ18.7 and [FeII]λ17.9 (cf. Table 1).

Another interesting result is that [FeII]λ26.0/[NeII]λ12.8 and [FeII]λ26.0/[SiII]λ34.8 are both a factor of $\simeq$1.7 lower than those observed in RCW103 (Oliva et al. 1998), while the density sensitive [FeII]λ17.9/λ26.0 ratio is similar in the two objects. This result indicates that IC443 has a lower Fe gas phase abundance than RCW103 where the Fe/Ne and Fe/Si relative abundances were found to be close to their solar values. This difference may reflect intrinsic differences in the ISM total element abundances or, more likely, imply that the shock in IC443 is slower and therefore less effective in destroying the Fe–bearing grains. This last possibility is also supported by other "speedometers", i.e. the line surface brightness and the [NeIII]/[NeII] ratio which are lower by a factor of 7 and 1.6, respectively.

3. Discussion

The data presented above strongly suggest that most of the 12 and 25 μm flux from the NE rim of IC443 is due to ionic line emission rather than continuum emission from warm dust. We address here the following questions. Can this result be generalized to other radiative SNRs? Are there other lines which may severely contaminate IRAS measurements of this and other remnants?

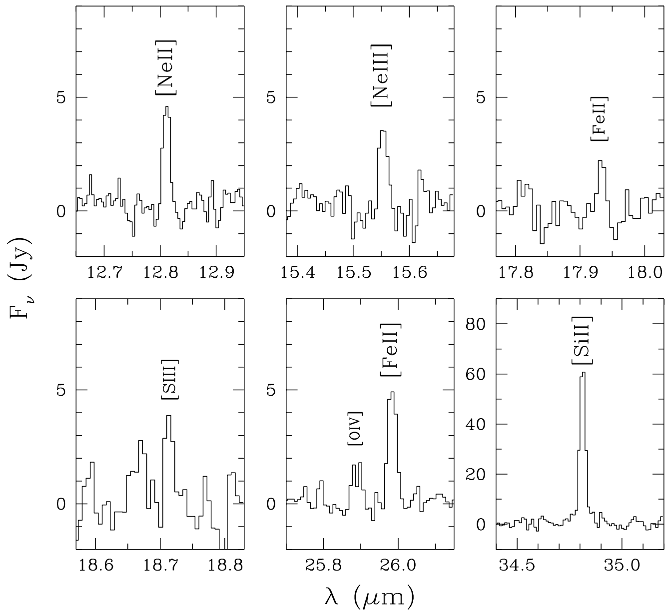

Fig. 2. Selected sections of the SWS01 spectrum of the north–east rim of IC443, note that each spectral segment has been "continuum subtracted" (using a $\leq$2 degree polynomial) to remove instrumental offsets and drifts. The position of instrument aperture is shown in Fig. 1.

Table 1. Observed ISO line fluxes

Line	Flux$^{(1)}$	Slit$^{(2)}$	Σ–IRAS$^{(3)}$		
			12 μm	25 μm	60 μm
[NeII]λ12.81	18 (3)	14 × 27	20	–	–
[NeIII]λ15.56	10 (2)	14 × 27	–	–	–
[FeII]λ17.93	4 (1)	14 × 27	–	2	–
[SIII]λ18.71	4 (2)	14 × 27	–	3	–
[OIV]λ25.88	3 (1)	14 × 27	–	3	–
[FeII]λ25.98	8 (1)	14 × 27	–	10	–
[SiII]λ34.8	52 (7)	20 × 33	–	–	2
Observed IRAS fluxes^a			10	10	60

$^{(1)}$ Observed line flux, units of 10^{-16} W m^{-2}, errors are given in parenthesis

$^{(2)}$ Size (in arcsec) of the SWS apertures

$^{(3)}$ Equivalent surface brightness in the IRAS bands, units of 10^{-8} W m^{-2} sr^{-1}

^{a} Observed IRAS surface brightness at the position of the SWS aperture, estimated from Fig. 30a of A89, see also Fig. 1.

3.1. The IRAS 12 and 25 μm emission from other SNRs

The easiest and most direct estimate of the line contribution to the IRAS fluxes requires a measurement of the FIR line intensity from the whole SNR. This is virtually impossible in IC443 and other radiative remnants in the Galaxy because of their very large projected sizes, but is feasible in the LMC where e.g. the remnant N49 has been mapped with SWS by Oliva et al. (in preparation). They find a total [NeII]λ12.8 line intensity of $2\,10^{-14}$ W m^{-2} and equal, within the errors, to the F(12μm)=2.2 10^{-14} W m^{-2} IRAS flux reported by Graham et al. (1987).

For remnants where direct measurements of FIR lines is not available, a reasonable estimate of their fluxes can be obtained by scaling optical line measurements using available ISO spectral observations of radiative SNRs, namely IC443 (this paper), RCW103 (Oliva et al. 1998) and N49 (Oliva et al. in preparation). These indicate that the [NeII] and [FeII]+[SIII]+[OIV] line contribution to the 12 and 25 μm filters are both roughly equal to the flux of Hβ. Unfortunately, relatively few optical spectrophotometric observations of SNRs are available in the literature and are altogether missing for several important radiative remnants such as W44 and W49B. Nevertheless, the SW filament of RCW86 has $\Sigma(\mathrm{H}\beta) \simeq 4\,10^{-7}$ (Leibowitz & Danziger 1983) and very similar to the $\Sigma \simeq 3\,10^{-7}$ W m^{-2} sr^{-1} IRAS 12 and 25 μm fluxes found by A89. Similarly, the NE filament of the Cygnus Loop has $\Sigma(\mathrm{H}\beta) \simeq 1\,10^{-7}$ (Fesen et al. 1982) and close to the IRAS surface brightness $\Sigma \simeq 8\,10^{-8}$ W m^{-2} sr^{-1} (A89). These results suggest, therefore, that lines account for most of the IRAS 12 and 25 μm emission from line emitting filaments of radiative SNRs.

Another interesting exercise is to compare optical line and IRAS fluxes in a younger remnant such as the Kepler SNR for which accurate line photometric measurements are available (D'Odorico et al. 1986). The total Hβ emission from the whole remnant is $2.9\,10^{-15}$ W m^{-2} and only 2% and 0.6 % of the IRAS flux in the 12 and 25 μm bands, respectively. This indicates, therefore, that line contamination is negligible in this object.

3.2. Contamination from other lines

The positions of the most important lines are marked in Fig. 3 where one can see that [SiII]λ34.8, although very prominent in SNRs, does not contribute significantly because it falls at a wavelength where IRAS was virtually blind. The same applies to [NeIII]λ15.6 which has an intensity comparable to [NeII] but falls in the hole between the 12 and 25 μm filters.

The possible contribution of [OI]λ63.0 to the IRAS 60 μm band was already pointed out by Burton et al. (1990) who observed this line in the southern ("molecular") rim of IC443 using a 33" aperture spectrometer on the KAO and found line surface brightnesses a factor of $\sim$2 larger than those measured by IRAS. On the other hand, however, ISO–LWS measurements of [OI]λ63.0 through a $\oslash$ 80" aperture centered on the optical filaments of W44 (Reach & Rho 1996) yield a line surface brightness a factor of $\simeq$2.5 *lower* than the IRAS 60 μm flux[1] indicating, therefore, that the contamination by [OI] is relatively unimportant, at least in this remnant.

[1] Note that the "continuum" in the LWS spectra of W44 by Reach & Rho (1996) is most probably an instrumental artifact, its level being 10 times brighter than the IRAS 60 μm background+source flux

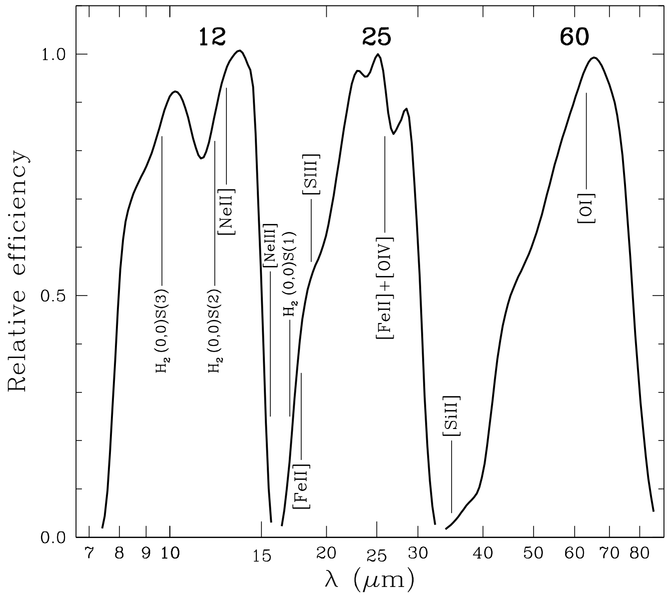

Fig. 3. Instrumental spectral response of IRAS (adapted from Fig. 2 of Neugebauer et al. 1984) with overlaid the positions of the brightest ionic, atomic and molecular lines.

The H_2 rotational lines could strongly affect the 12 μm band and may explain why the S(12)/S(25) ratio is a factor of $\simeq$2.5 larger on the southern rim of IC443, i.e. at $\simeq 06^h 14^m 40^s$ +22^{o}23' (cf. Fig. 1). This region is a well known powerful source of H_2 (1,0)S(1)λ2.12 line emission (Burton et al. 1988) whose spatial distribution closely resembles the IRAS 12 μm contours. Ground–based observations of the (0,0)S(2)λ12.3 rotational transition were obtained by Richter et al. (1995) who measured a line flux $\simeq$10 times brighter than (1,0)S(1)λ2.12. Assuming a constant I(λ12.3)/I(λ2.12) ratio over the large area mapped in the latter transition by Burton et al. (1988) yields an average line surface brightness of about $1.5\,10^{-7}$ W m^{-2} sr^{-1} or 1/3 of the IRAS 12 μm peak surface brightness. Considering that the H_2 spectrum of IC443 is remarkably similar to that of Orion peak1 (e.g. Richter et al. 1995) one then expects similar fluxes in the (0,0)S(3)λ9.66 and (0,0)S(2)λ12.3 lines (Parmar et al. 1994) or, equivalently, that the two lines should account for about 2/3 of the IRAS 12 μm flux.

Finally, it should be noted that IRAS was virtually blind to the H_2(0,0)S(1)λ17.0 line (cf. Fig. 3) while the highly forbidden ground state transition (0,0)S(0)λ28.2 is most probably too weak to significantly contaminate the 25 μm IRAS band (cf. e.g. Fig. 2 of Oliva et al. 1998).

4. Conclusions

An ISO–SWS spectrum of IC443 has revealed prominent [NeII] and [FeII] line emission which, together with [SIII] and [OIV], account for most of the observed IRAS flux in the 12, 25 μm bands. Simple arguments indicate that this is probably the case in other radiative SNRs and this result suggests that the unusually blue IRAS colours of radiative SNRs simply reflect line contamination, rather than a large population of small grains which are otherwise required to explain the warmer “continuum” emission. Available ground based data also indicate that S(2), S(3) rotational lines of H_2 contribute to a large fraction of the IRAS 12 μm emission from the southern rim of IC443.

The relative fluxes of the ionic lines detected by ISO yield a $\simeq$0.6 $\times$ solar Fe gas–phase relative abundance which is significantly lower than that found in the much more powerful RCW103 supernova remnant. This may imply that the shock in IC443 is slower and thus less effective in destroying the Fe–bearing grains. This scenario is also supported by the lower line surface brightness and [NeIII]/[NeII] ratio which both indicate a lower shock speed in IC443.

Acknowledgements. We thanks the referee, R. Arendt, for useful comments and criticisms.
E. Oliva acknowledges the partial support of the Italian Space Agency (ASI) through the grant ARS–98–116/22.
SWS and the ISO Spectrometer Data Center at MPE are supported by DLR (formerly DARA) under grants 50–QI–8610–8 and 50–QI–9402–3.

References

Arendt R.G., 1989, ApJS 70, 1 (A89)
Arendt R.G., Dwek E., Leisawitz D., 1992, ApJ 400, 562
Braun R., Strom R.G., 1986, A&A 164, 193
Burton M.G., Geballe T.R., Brand P.W.J.L., Webster A.S., 1988 231, 617
Burton M.G., Hollenbach D.J., Haas M.R., Erickson E.F., 1990, ApJ 355, 197
D'Odorico S., Bandiera R., Danziger I.J., Focardi P., 1986, AJ 91, 1382
Dwek E., 1987, ApJ 322, 812
Dwek E., Petre R., Szymkowiak A., Rice W.L., 1987, ApJL 320, L27
Draine B.T., 1981, ApJ 245, 880
Fesen R.A., Kirshner R.P., 1980, ApJ 242, 1023
Fesen R.A., Blair W.P., Kirshner R.P., 1982, ApJ 262, 171
Graham J.R., Evans A., Albinson J.S., Bode M.F., Meikle W.P.S., 1987, ApJ 319, 126
Leibowitz E.M., Danziger I.J., 1983, MNRAS 204, 273
Mufson S.L., McCollough M.L., Dickel J.R., Petre R., White R., Chevalier R., 1986, AJ 92, 1349
Neugebauer G., Habing H. J., van Duinen R., Aumann H. H., Baud B., Beichman C. A., Beintema D. A., Boggess N., Clegg P. E., de Jong T., Emerson J. P., Gautier T. N., Gillett F. C., Harris S., Hauser M. G., Houck J. R., Jennings R. E., Low F. J., Marsden P. L., Miley G., Olnon F. M., Pottasch S. R., Raimond E., Rowan-Robinson M., Soifer B. T., Walker R. G., Wesselius P. R., Young E., 1984, ApJL 278, L1
Oliva E., Moorwood A.F.M., Drapatz S., Lutz D., Sturm E., 1998, submitted to A&A
Ostriker J.P., Silk J., 1973, ApJL 184, L113
Parmar P.S., Lacy J.H., Achtermann J.M., 1994, ApJ 430, 786
Reach W.T., Rho J., 1996, A&A 315, L277
Richter M.J., Graham J.R., Wright G.S., Kelly D.M., Lacy J.H., 1995, ApJL 449, L83